

## ORIGINAL ARTICLE

## MicroRNA-149 targets GIT1 to suppress integrin signaling and breast cancer metastasis

S-H Chan<sup>1,11</sup>, W-C Huang<sup>1,2,11</sup>, J-W Chang<sup>1</sup>, K-J Chang<sup>3</sup>, W-H Kuo<sup>3</sup>, M-Y Wang<sup>3</sup>, K-Y Lin<sup>4</sup>, Y-H Uen<sup>4</sup>, M-F Hou<sup>5</sup>, C-M Lin<sup>1</sup>, T-H Jang<sup>1</sup>, C-W Tu<sup>6</sup>, Y-R Lee<sup>7</sup>, Y-H Lee<sup>8</sup>, M-T Tien<sup>9</sup> and L-H Wang<sup>1,2,10</sup>

Metastasis is the predominant cause of death in breast cancer patients. Several lines of evidence have shown that microRNAs (miRNAs) can have an important role in cancer metastasis. Using isogenic pairs of low and high metastatic lines derived from a human breast cancer line, we have identified miR-149 to be a suppressor of breast cancer cell invasion and metastasis. We also identified GIT1 (G-protein-coupled receptor kinase-interacting protein 1) as a direct target of miR-149. Knockdown of GIT1 reduced migration/invasion and metastasis of highly invasive cells. Re-expression of GIT1 significantly rescued miR-149-mediated inhibition of cell migration/invasion and metastasis. Expression of miR-149 impaired fibronectin-induced focal adhesion formation and reduced phosphorylation of focal adhesion kinase and paxillin, which could be restored by re-expression of GIT1. Inhibition of GIT1 led to enhanced protein degradation of paxillin and  $\alpha 5\beta 1$  integrin via proteasome and lysosome pathways, respectively. Moreover, we found that GIT1 depletion in metastatic breast cancer cells greatly reduced  $\alpha 5\beta 1$ -integrin-mediated cell adhesion to fibronectin and collagen. Low level of miR-149 and high level of GIT1 was significantly associated with advanced stages of breast cancer, as well as with lymph node metastasis. We conclude that miR-149 suppresses breast cancer cell migration/invasion and metastasis by targeting GIT1, suggesting potential applications of the miR-149-GIT1 pathway in clinical diagnosis and therapeutics.

Oncogene (2014) 33, 4496–4507; doi:10.1038/onc.2014.10; published online 10 March 2014

## INTRODUCTION

Metastasis is the major obstacle for treatment of cancer, accounting for over 90% of cancer patients' death including breast cancer.<sup>1</sup> Metastasis is an intricate, multistep process involving escape from the primary tumor site, local invasion, intravasation, survival in the systemic circulation, extravasation into distant organs and finally successful colonization and outgrowth at the secondary sites.<sup>2,3</sup>

MicroRNAs (miRNAs), a class of small noncoding regulatory RNA, have been reported to affect different steps of cancer metastasis in either a positive or negative way, depending on the function of their target genes.<sup>4–6</sup>

Previous studies have shown that interactions between tumor cells and their surrounding extracellular matrices have a crucial role in multiple aspects of tumor progression including metastasis.<sup>7,8</sup> The binding of extracellular matrix components such as fibronectin, collagen and laminin to integrins leads to the formation of focal adhesions, which link extracellular matrix to the intracellular actin cytoskeleton. Focal adhesion signaling contributes to cancer metastasis by promoting cancer cell migration, invasion, survival and angiogenesis.<sup>7,9–11</sup>

GIT1, the G-protein-coupled receptor kinase-interacting protein 1, has multiple domains, including ARFGAP, Spa2 homology, three ankyrin repeats, coiled coil and paxillin-binding domains.<sup>12</sup> GIT1 has been known to have a central role in regulating focal adhesion, cell migration, lamellipodia formation and

endocytosis.<sup>13,14</sup> In migrating cells, GIT1 is found to be localized with paxillin and focal adhesion kinase (FAK) at focal adhesion points and also has been shown to bind to PIX, a guanine exchange factor for Rac1/Cdc42, to form a GIT1-PIX-p21-activated kinase (PAK) complex to regulate positively cell protrusion at leading edges. However, GIT1's role in cancer metastasis is yet to be determined.

In this study, we established highly metastatic breast cancer lines by *in vivo* selection from the MDA-MB-231 line and identified a novel miRNA, miR-149, that could directly target GIT1 expression to suppress integrin signaling and breast cancer migration/invasion and metastasis.

## RESULTS

miRNA microarray profiling identified miRNAs differentially expressed in the *in vivo*-selected metastatic breast cancer cells versus their parental cells

To identify novel miRNAs that are involved in regulating breast cancer metastasis, we attempted to select highly metastatic cells from seven human breast cancer lines using an *in vivo* model. One million cells from MCF-7, T-47D, SK-BR3, BT-549, Hs578T, MDA-MB-453 and MDA-MB-231 were injected individually into the tail vein of severe-combined immunodeficient mice (Supplementary Figure 1). After two rounds of *in vivo* selection from lung metastases (described in Materials and methods and

<sup>1</sup>Institute of Molecular and Genomic Medicine, National Health Research Institute, Miaoli, Taiwan; <sup>2</sup>Department of Life Science, National Central University, Taoyuan, Taiwan; <sup>3</sup>Department of Surgery, National Taiwan University Hospital, Taipei, Taiwan; <sup>4</sup>Chi Mei Medical Center, Department of Medical Research, Tainan, Taiwan; <sup>5</sup>Department of Surgery, Kaohsiung Medical University Chung-Ho Memorial Hospital, Kaohsiung, Taiwan; <sup>6</sup>Department of Surgery, Chiayi Christian Hospital, Chiayi, Taiwan; <sup>7</sup>Department of Medical Research, Chiayi Christian Hospital, Chiayi, Taiwan; <sup>8</sup>Department of Pathology, National Taiwan University Hospital Hsin-Chu Branch, Hsinchu, Taiwan; <sup>9</sup>Biomedical Technology and Device Research Laboratories, Industrial Technology Research Institute, Hsinchu, Taiwan and <sup>10</sup>Department of Microbiology, Mount Sinai School of Medicine, New York, NY, USA. Correspondence: Dr L-H Wang, Institute of Molecular and Genomic Medicine, National Health Research Institute, 35 Keyan Road, Zhunan Town, 35053 Miaoli, Taiwan. E-mail: lu-hai.wang@nhri.org.tw

<sup>11</sup>These authors contributed equally to this work.

Received 9 July 2013; revised 28 November 2013; accepted 29 November 2013; published online 10 March 2014

Supplementary Figure 1), we successfully isolated three highly metastatic sublines from MDA-MB-231 parental cells ('231 parental cells') and named them IV2-1, IV2-2 and IV2-3, respectively. The rest of breast cancer lines failed to establish highly metastatic sublines under such conditions.

*In vitro* invasion assay confirmed that those IV2 lines exhibited higher invasiveness than the parental 231 cells (Supplementary Figure 2). *In vivo* metastasis assay showed that when IV2-1 cells were inoculated into fat pads of the severe-combined immunodeficient mice, they exhibited more aggressive lung and lymph node metastasis compared with the parental cells (Supplementary Figure 3 and Supplementary Table 1).

Next, we compared the miRNA expression patterns between the parental 231 and IV2 sublines to identify differentially expressed miRNAs possibly associated with the aggressive lung metastasis using miRNA array analysis. Hierarchical clustering of miRNA expression profiles revealed that a group of miRNAs were differentially expressed in the IV2 sublines (Supplementary Figure 4). We searched for the potential 'metastasis suppressor miRNAs' by identifying those downregulated at least threefold in all three IV2 sublines (Supplementary Table 2). The miRNAs thus identified were confirmed by Taqman quantitative real-time polymerase chain reaction (qRT-PCR) (Supplementary Figure 5). The results showed that miRNA-149 was consistently downregulated in all the metastatic IV2 sublines (Figures 1a and b).

#### miR-149 suppresses breast cancer cell migration and invasion *in vitro*

Overexpression of pre-miR-149 did not affect cell proliferation *in vitro* (Supplementary Figure 6), but suppressed cell migration by threefold and invasion by fivefold in the IV2-1 and IV2-2 cells, and the inhibition was reverted substantially by co-transfection with anti-miR-149 (Figure 1c). Similar results were obtained in the invasive Hs578T cells (Figure 1c and Supplementary Figure 7). Taken together, we showed that miR-149 suppressed cell migration and invasion of metastatic breast cancer cells.

#### miR-149 functions as a metastasis suppressor *in vivo*

Next, we tested if miR-149 functions as a metastasis suppressor in a mouse model. The control IV2-1, pre-miR-149-transfected IV2-1 and the parental 231 cells were injected into immunodeficient mice via tail veins. After 45 days, lung metastasis status of the mice was checked by histological examination. Hematoxylin and eosin (H&E) staining of lung sections revealed that pre-miR-149-transfected IV2-1 showed a lower metastatic ability compared with the control IV2-1 cells (Figures 1d and e). The parental cells had the lowest metastatic ability (Figures 1d and e). Furthermore, we showed that reduced lung metastasis of the pre-miR-149-transfected IV2 cells appeared because of impaired lung targeting ability 24 h after injection (Supplementary Figure 9).

We conclude that miR-149 functions as a novel suppressor of breast cancer cell metastasis.

#### GIT1 is a direct target of miR-149

We explored the mechanism underlying the suppressive role of miR-149 in breast cancer cell invasion and metastasis. Two miRNAs target prediction algorithms, Targetscan and Pictar, were used to search for the putative targets of miR-149. We focused on genes related to cell motility and adhesion. Guided by Gene Ontology analysis, we found one potential target, GIT1. Previous studies have demonstrated that GIT1 is a cell migration- and focal adhesion-related scaffold protein.<sup>13–15</sup> To test if that GIT1 is a direct target of miR-149, a luciferase reporter containing the GIT1 3'-untranslated region (UTR) harboring a conserved miR-149 binding site was constructed (Figure 2a). The reporter assay showed that pre-miR-149 significantly reduced the luciferase

activity in the IV2-1 cells and this inhibition could be significantly reduced by co-transfection with the anti-miR-149. Mutation of the miR-149 binding site abolished the inhibition by miR-149 (Figures 2a and b).

Next, we showed that overexpression of pre-miR-149 could reduce the endogenous GIT1 expression in IV2-1, parental 231 and Hs578T cells and this inhibition could be reverted by co-transfection with anti-miR-149 (Figure 2c). In addition, we showed that miR-149 could suppress GIT1 expression at the mRNA level (Supplementary Figure 10). Furthermore, inhibition of the endogenous miR-149 by anti-miR-149 or miR-149 sponge, an effective binder of its target miRNA (Supplementary Figure 11), increased the endogenous GIT1 protein expression in the parental 231 cells (Figure 2d). Analysis of the endogenous GIT1 level in parental 231 line and IV2 sublines showed that the IV2 sublines had twofold increase of GIT1 expression at RNA and protein levels compared with the parental 231 cells (Figure 2e).

Taken together, our results demonstrate that miR-149 directly suppresses GIT1 expression in breast cancer cells.

#### Low miR-149 and high GIT1 level correlates with the invasive phenotype of breast cancer cell lines

Next, we examined the correlation of miR-149 and GIT1 in the invasiveness of breast cancer cell lines. We found that low miR-149 and high GIT1 level was associated with the invasive phenotype of breast cancer cell lines (Figure 3a). Interestingly, MCF-10A, a normal breast cell line, had very low level of miR-149 and modest GIT1 expression, suggesting that miR-149-GIT1 regulation might not have an important role in MCF-10A cell migration and invasion. Importantly, we found that miR-149 level was inversely correlated with GIT1 protein and mRNA level in those breast cancer lines (Figure 3b).

#### Knockdown of the endogenous GIT1 expression by siRNAs impairs cell migration and invasion

To assess the role of GIT1 in metastasis, we tested if inhibition of GIT1 would affect cell migration and invasion of the IV2 cells. Transfection of three small interfering RNAs (siRNAs) against different coding regions of GIT1 effectively suppressed GIT1 but not GIT2 expression (Figure 4a and Supplementary Figure 12), and also inhibited migration/invasion of the cells (Figure 4b), whereas cell proliferation under such condition was not affected (Supplementary Figure 13). Similar results were obtained in the Hs578T cells (Supplementary Figure 14). Thus, inhibition of GIT1 impairs migration/invasion, but not proliferation, of invasive breast cancer cells.

#### Re-expression of GIT1 partially reverses miR-149-mediated suppression of migration and invasion

To test whether miR-149-induced inhibition of cell migration and invasion could be reversed by restoration of GIT1 expression, we transfected miR-149-expressing IV2-1 cells with a GIT1 expression construct (Figure 4c). Re-expression of GIT1 significantly reversed miR-149-mediated inhibition of cell migration and invasion (Figure 4d). However, overexpression of GIT1 in the IV2-1 cells did not further enhance their migration and invasion, suggesting that the threshold level of GIT1 was functionally sufficient (Figure 4d). In addition, mutation of the ArfGAP domain of GIT1 (R39K mutant) did not affect the ability of GIT1 to rescue the miR-149-mediated inhibition, suggesting that ArfGAP activity of GIT1 is not required for GIT1-mediated migration and invasion of invasive breast cancer cells (Supplementary Figure 15).

#### Re-expression of GIT1 partially rescues miR-149-suppressed lung metastasis

Next, we examined whether re-expression of GIT1 could restore miR-149-suppressed lung metastasis (Figure 1d). The result

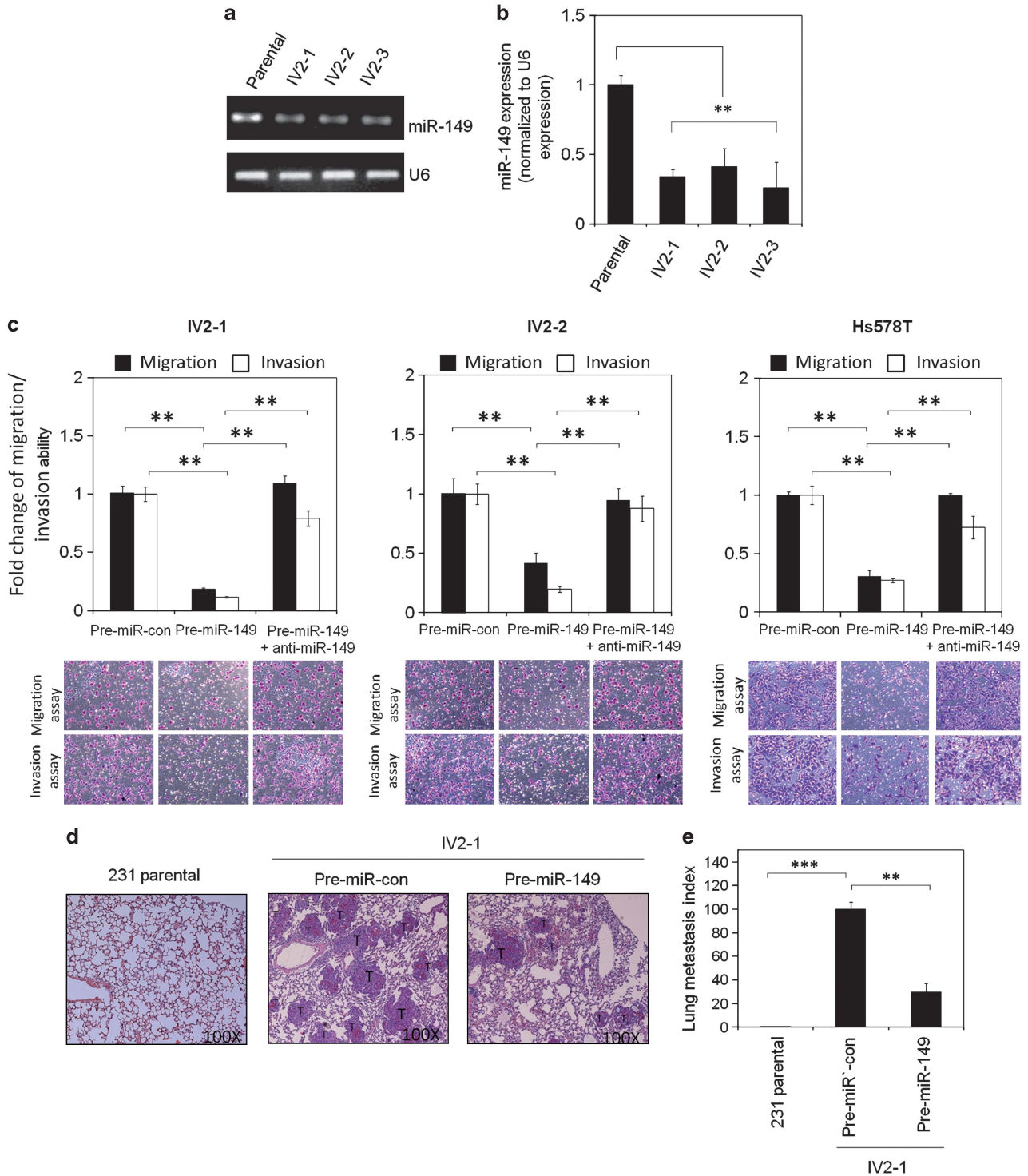


**Figure 1.** miR-149 is downregulated in highly metastatic IV2 sublines and suppresses breast cancer cell migration, invasion and metastasis. **(a and b)** The expression level of miR-149 in three IV2 sublines was measured using conventional RT-PCR and qRT-PCR. **(c)** Analysis of the effect of miR-149 on IV2 and Hs578T cell migration and invasion using Boyden chamber assay. Quantitative data are shown by histograms and representative photographs of the migrated/invaded cells from different treatments are shown. **(d)** H&E staining of mouse lung tissues 45 days after tail vein injection of pre-miR-149-transfected IV2-1, the control IV2-1 cells and the parental 231 cells. Transfection efficiency was monitored using FAM-labeled pre-miR-149 (Supplementary Figure 8). T indicates metastatic tumor areas. **(e)** The mean of lung metastasis index in the lung from five mice in each group. Lung metastasis index was calculated as the following: metastatic tumor areas/total lung areas. All the *in vitro* experiments were performed in triplicates and repeated three times. \*\* $P < 0.01$  and \*\*\* $P < 0.001$  compared with controls or between the indicated groups.

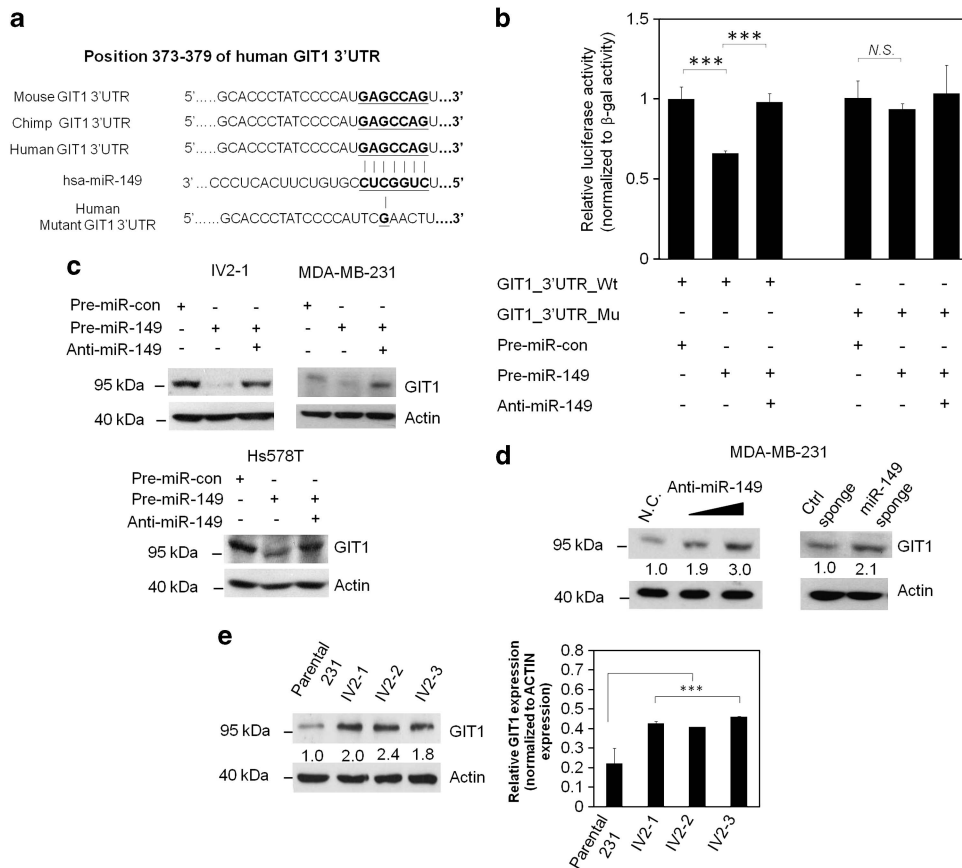


**Figure 2.** GIT1 is a direct target of miR-149 in breast cancer cells. **(a)** Schematics of highly conserved miR-149 binding site in human GIT1 3'-UTR. **(b)** Luciferase activity of the wild-type (Wt) and the mutant (Mu) GIT1 3'-UTR reporter constructs in the presence of miR-149. **(c)** The effect of pre-miR-149 transfection on GIT1 protein expression in IV2-1, parental 231 and Hs578T cells was analyzed by western blotting. **(d)** Effect of inhibition of endogenous miR-149 on GIT1 expression either by transfection of anti-miR-149 or by stable expression of miR-149 sponge construct in parental 231 cells. **(e)** Analysis of the endogenous protein and mRNA expression of GIT1 in parental 231 line and three IV2 sublines. All the *in vitro* experiments were performed in triplicates and repeated three times. \*\*\* $P < 0.001$  compared with controls or between indicated groups. NC, negative control; NS, no significance.

showed that miR-149 reduced 90% of IV2-induced lung metastasis and re-expression of GIT1 restored lung metastasis to 35% of the control (Figures 4e and f). In addition, overexpression of GIT1 in IV2 cells did not further enhance their lung metastasis, which was consistent with the *in vitro* findings of invasion assay.

Taken together, we have demonstrated that the miR-149/GIT1 signaling axis has an important role in breast cancer metastasis.

Inhibition of GIT1 expression by miR-149 or GIT1 siRNAs impairs focal adhesions and focal adhesion signaling, which is significantly rescued by re-expression of GIT1

Previous studies have shown that GIT1 binds to paxillin and is colocalized at focal adhesions.<sup>14,15</sup> Several lines of evidence have suggested that fibronectin-induced focal adhesion signaling is crucial for breast cancer progression and metastasis.<sup>16</sup> We thus tested if inhibition of GIT1 expression could impair focal adhesion signaling in the metastatic IV2 cells.

The result showed that inhibition of GIT1 expression by pre-miR-149 significantly reduced phosphorylation of FAK at Y397 and Y861 and paxillin at Y118 (Figure 5a). The miR-149-impaired phosphorylation of paxillin was likely in part due to the decrease of its protein level, which was, however, not the case for FAK (Figure 5a). Inhibition of miR-149 by anti-miR-149 could reverse miR-149-mediated suppression of FAK and paxillin phosphorylation, as well as the protein level of paxillin (Figure 5a). Re-expression of GIT1 in the miR-149-expressing IV2-1 cells

restored the phosphorylation level of FAK, and the paxillin and the protein level of paxillin (Figure 5b). Moreover, immunofluorescence staining of focal adhesion complexes with vinculin antibody revealed that depletion of GIT1 by miR-149 reduced focal adhesions at the peripheral of IV2-1 cells by 2.5-fold as compared with the control, which could be restored by re-expression of GIT1 (Figures 5c and d).

We further asked whether inhibition of the endogenous GIT1 using GIT1 siRNA would recapitulate the effect of miR-149. Indeed, depletion of GIT1 decreased the phosphorylation of FAK and paxillin and reduced the protein level of paxillin (Figure 5e). Likewise, focal adhesions of the GIT1-depleted IV2 cells were decreased by about 2.5-fold as compared with the control (Figures 5f and g).

Collectively, the above results suggest that miR-149 impairs fibronectin-induced focal adhesion formation of the metastatic IV2 cells through targeting GIT1 expression. Our findings provide first evidence and insight that depletion of GIT1 impairs focal adhesion signaling in metastatic breast cancer cells.

Depletion of GIT1 leads to enhanced proteasome-mediated degradation of paxillin

Inhibition of GIT1 expression by miR-149 or GIT1 siRNA reduced paxillin at the protein level prompted us to question whether depletion of GIT1 led to enhanced protein degradation of paxillin as its mRNA was not affected (Figure 6a). The result showed that

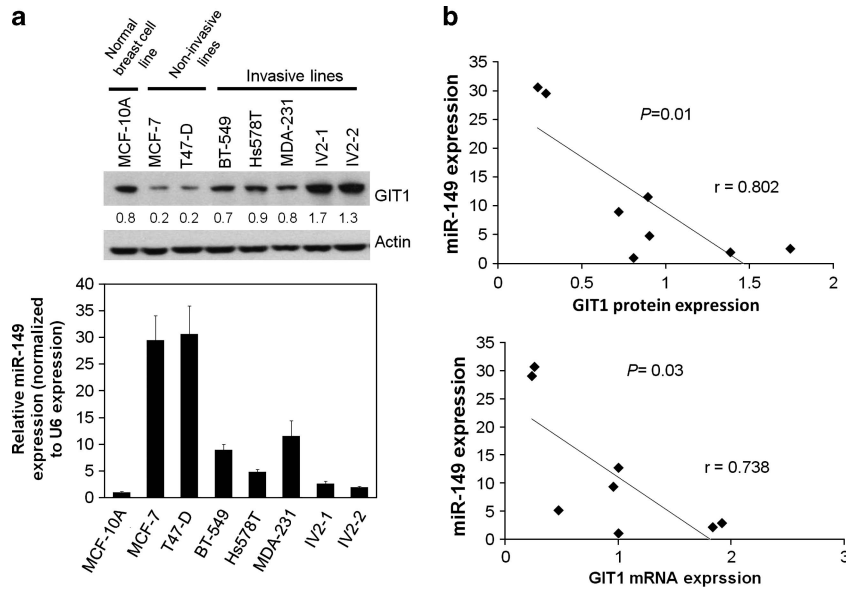


**Figure 3.** miR-149 and GIT1 expression are associated with the invasive phenotype of breast cancer cell lines. **(a)** miR-149 and GIT1 expression among breast cancer lines was analyzed by western blotting and Taqman qRT-PCR, respectively. Triple-negative breast cancer cell lines (TNBCs) with invasive phenotype, BT-549, Hs578T and MDA-MB-231, expressed lower miR-149 levels and higher GIT1 levels as compared with estrogen receptor (ER)-positive breast cancer lines with low invasive phenotype such as MCF-7 and T-47D. Low level of miR-149 and modest level of GIT1 were found in normal breast epithelial line, MCF-10A. **(b)** Correlation analysis of miR-149 and GIT1 in breast cancer cell lines. All the *in vitro* experiments were performed in triplicates and repeated three times.

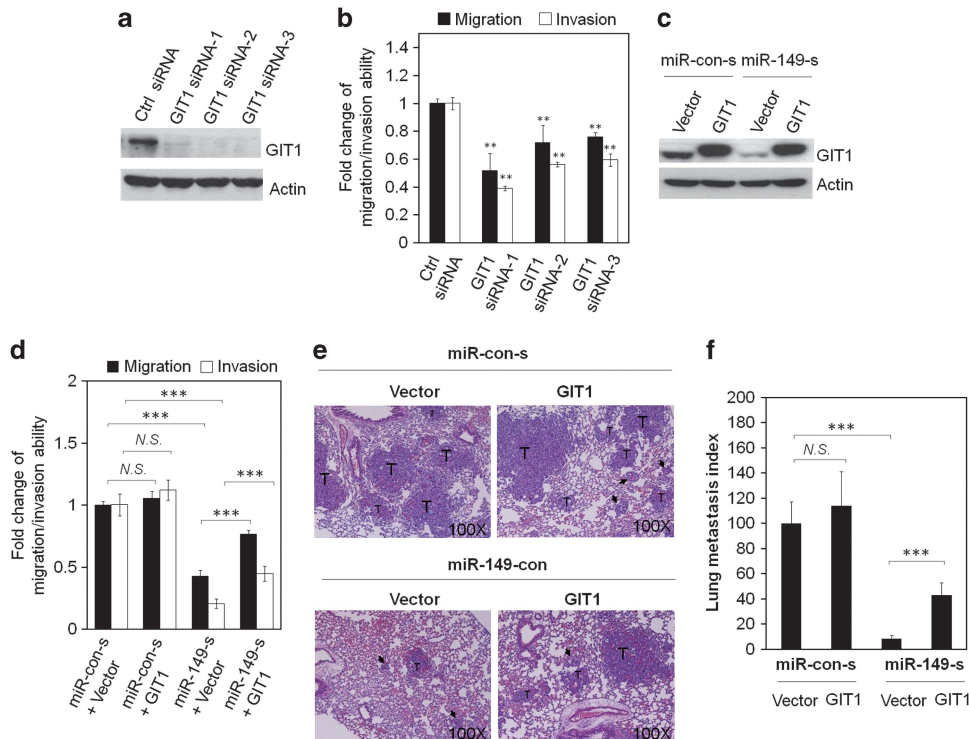


**Figure 4.** miR-149-dependent inhibitory effect on cell migration/invasion and metastasis could be partially reversed by re-expression of GIT1 *in vitro* and *in vivo*. **(a)** Western blotting analysis of three different siRNAs against GIT1 in IV2-1 cells. **(b)** Analysis of cell migration and invasion in GIT1 knockdown IV2-1 cells similar to that in Figure 1. **(c)** Analysis of GIT1 protein level in miR-149-expressing IV2-1 cells with or without GIT1 re-expression. **(d)** The effect of GIT1 re-expression in miR-149-expressing IV2-1 cells on cell migration and invasion. **(e)** Image of H&E staining of mouse lung tissues 45 days after tail vein injection of IV2-1 cells with the indicated treatments. T indicates metastatic tumor areas and black arrows indicate the area of micrometastasis. **(f)** The mean of lung metastasis index in the lung from five mice in each group. The control (Ctrl) or miR-149-expressing IV2-1 cells with or without exogenous GIT1 expression were injected into tail veins of immunodeficient mice. After 45 days, the mice were killed and examined for lung metastasis by histological analysis. Lung metastasis index was calculated as follows: metastatic tumor areas/total lung areas. All the *in vitro* experiments in **(a-d)** were performed in triplicates and repeated three times. \*\* $P < 0.01$  and \*\*\* $P < 0.001$  compared with Ctrl or between indicated groups. NS, no significance.

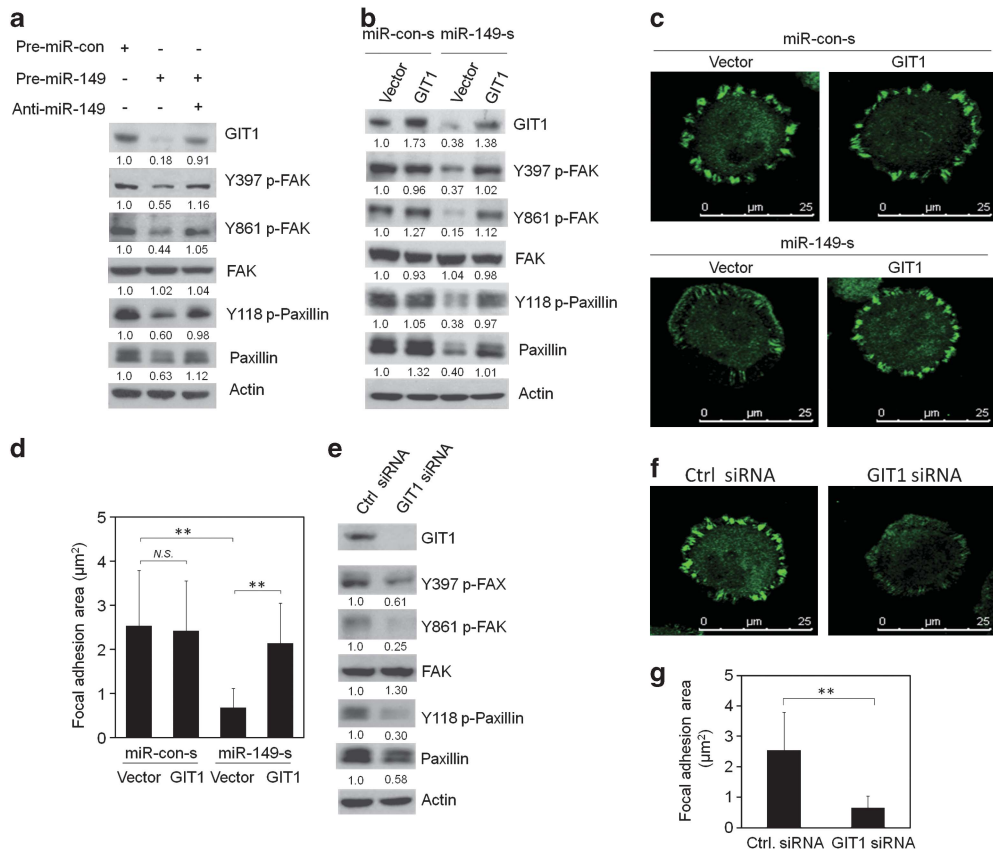


**Figure 5.** Inhibition of GIT1 expression by miR-149 or GIT1 siRNAs suppresses phosphorylation (p) of FAK and paxillin and focal adhesion formation of metastatic IV2 cells. **(a)** Analysis of focal adhesion signaling molecules in pre-miR-149-transfected IV2-1 cells. IV2-1 cells were transfected with pre-miR-149 or a combination of pre-miR-149 and anti-miR-149. After 48 h, cells were trypsinized and seeded on fibronectin-coated dishes for 90 min and then total proteins were extracted and subjected to western blotting analysis. **(b)** The effect of re-expressing GIT1 on focal adhesion signaling molecules in miR-149-expressing IV2-1 cells. **(c)** Analysis of IV2-1 cells with the indicated treatments for focal adhesions by immunostaining of vinculin. **(d)** Quantitative data of focal adhesion areas of IV2-1 cells from the indicated treatment are shown by histograms. One hundred cells were analyzed in each group. **(e)** Effect of GIT1 Knockdown on focal adhesion signaling molecules in IV2-1 cells. **(f)** Analysis of the effect of GIT1 knockdown in IV2-1 cells for focal adhesions by immunostaining of vinculin. **(g)** Quantitative data of focal adhesion areas of IV2 cells from the indicated treatment are shown by histograms. One hundred cells were analyzed in each group. All experiments were performed in triplicates in each experiment and repeated three times.  $**P < 0.01$  compared with controls (Ctrls) or between indicated groups. NS, no significance.

8 h of treatment with the proteasome inhibitor MG132 in the GIT1-depleted cells restored the paxillin level to that of the control (Figure 6b), implying that GIT1 contributed to the stability of paxillin via preventing it from proteasome-mediated degradation. To confirm this, we performed degradation assay in cells treated with protein synthesis inhibitor cycloheximide. The result showed that paxillin stability was markedly decreased over the course of 8 h in GIT1-depleted cells (Figures 6c and d).

Taken together, depletion of GIT1 enhances proteasome-mediated degradation of paxillin and thus decreased its stability.

Depletion of GIT1 leads to enhanced lysosome-mediated protein degradation of  $\alpha 5\beta 1$  integrin

As paxillin binds to the cytoplasmic domain of  $\beta 1$  integrin upon fibronectin-induced focal adhesion formation,<sup>17</sup> we asked if depletion of GIT1 could similarly affect  $\beta 1$  integrin. Our data showed that the protein level of  $\beta 1$  integrin was significantly decreased in GIT1-depleted IV2-1 cells (Figure 6h) and it was not due to the decrease of mRNA (Figure 6g). We thus examined if GIT1 knockdown also enhanced protein degradation of  $\beta 1$  integrin. Integral membrane proteins such as integrins are known to be degraded in part via lysosome-mediated pathway.<sup>18</sup> Therefore, we treated GIT1-depleted IV2-1 cells with lysosomal inhibitors  $\text{NH}_4\text{Cl}$  and bafilomycin A.<sup>19</sup> The result showed that both

$\text{NH}_4\text{Cl}$  and bafilomycin A reduced about 50% of the effect of GIT1 depletion on  $\beta 1$  integrin level, whereas that of paxillin was not affected (Figure 6i). To confirm enhanced protein degradation of  $\beta 1$  integrin, we performed a similar degradation assay in cells treated with cycloheximide. The result showed that  $\beta 1$  integrin stability was significantly decreased over a course of 8 h in GIT1-depleted cells (Figure 6c and e). Thus, GIT1 appears to have a positive role in the stability of  $\beta 1$  integrin. As  $\beta 1$  integrin is known to form heterodimers with  $\alpha 5$  integrin to bind specifically to fibronectin,<sup>7</sup> we also checked the stability of  $\alpha 5$  integrin and observed the similar effect upon GIT1 depletion (Figures 6c, f and i). Finally, we showed that re-expression of GIT1 could restore paxillin and  $\alpha 5\beta 1$  integrin level in the pre-miR-149-transfected IV2-1 cells (Figure 6j).

Collectively, we conclude that GIT1 positively regulates fibronectin-induced focal adhesion formation of metastatic IV2 cells, at least in part, by maintaining the activation, as well as by maintaining the protein levels of paxillin and  $\alpha 5\beta 1$  of the integrin complexes.

Depletion of GIT1 impairs  $\alpha 5\beta 1$ -mediated cell adhesion to fibronectin and collagen

Next, we examined whether reduced  $\alpha 5\beta 1$  integrin level in GIT1-depleted IV2-1 cells could affect cell adhesiveness to fibronectin,

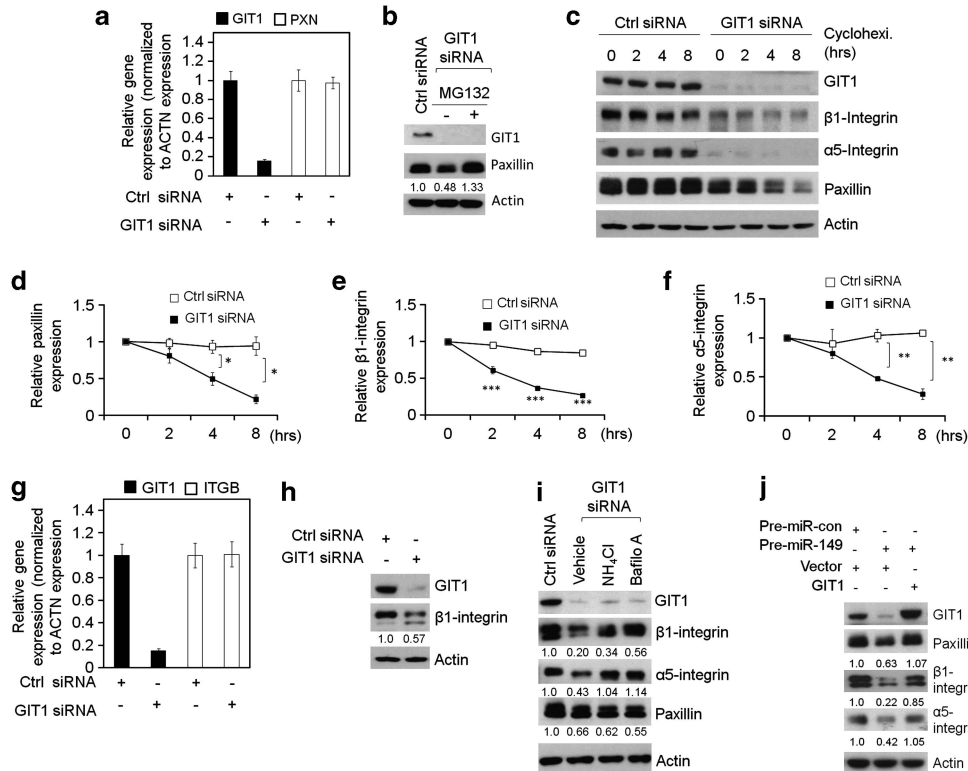


**Figure 6.** Depletion of GIT1 leads to enhanced protein degradation of paxillin (PXN) and  $\alpha 5\beta 1$  integrin in metastatic IV2 cells. **(a)** Quantitative PCR (qPCR) analysis showing no significant effect of GIT1 siRNA on paxillin mRNA level. **(b)** Eight hours of treatment with  $10 \mu\text{M}$  MG132 prevented the loss of paxillin in GIT1-depleted IV2-1 cells. **(c)** The levels of  $\alpha 5\beta 1$  integrin and paxillin in control (Ctrl) and GIT1-depleted IV2-1 cells treated with  $10 \mu\text{g/ml}$  cycloheximide (cyclohexi.) over the indicated periods. **(d)** Semiquantification of protein levels of paxillin and **(e and f)**  $\alpha 5\beta 1$  integrin in the Ctrl and GIT1-depleted IV2-1 cells. The protein level of  $\beta 1$  integrin is downregulated in GIT1-depleted IV2-1 cells. **(g)** qPCR analysis showing no significant effect of GIT1 siRNA on the  $\beta 1$  integrin (ITGB1) mRNA level. **(h)** The level of  $\beta 1$  integrin in GIT1-depleted IV2-1 cells. **(i)** Twenty-four hours of treatment with  $100 \text{ nM}$  bafilomycin A or  $20 \text{ mM}$   $\text{NH}_4\text{Cl}$  prevented about 50% of  $\beta 1$  integrin and almost 100% of  $\alpha 5$  integrin from protein degradation in GIT1-depleted IV2 cells. **(j)** Effect of re-expressing GIT1 on paxillin and  $\alpha 5\beta 1$  integrin level in pre-miR-149-transfected IV2-1 cells. All experiments were performed in triplicates in each experiment and repeated three times. \* $P < 0.05$ , \*\* $P < 0.01$  and \*\*\* $P < 0.001$  compared withCtrls.

the known ligand for  $\alpha 5\beta 1$  integrin, and other two non-cognate matrices, vitronectin and type IV collagen.

The result showed that depletion of GIT1 greatly reduced  $\alpha 5\beta 1$ -mediated cell adhesion to fibronectin and to collagen, although to a lesser extent, 30 and 60 min after seeding (Figures 7a and b). However, depletion of GIT1 did not affect adhesiveness of the IV2-1 cells to vitronectin (Figures 7a and b). Western blotting result confirmed GIT1 knockdown and reduced expression of paxillin and  $\alpha 5\beta 1$  integrin (Supplementary Figure 16). These results indicate that GIT1 is crucial for  $\alpha 5\beta 1$  integrin-mediated cell adhesion of metastatic breast cancer cells.

miR-149 and GIT1 expression significantly correlates with clinical stages and lymph node metastasis of breast cancer

Next, we investigated the clinical relevance of miR-149-GIT1 signaling in human breast cancers. The expression of miR-149 and GIT1 was analyzed in 157 human breast cancer specimens using Taqman qRT-PCR and conventional qRT-PCR, respectively. All the cancer specimens were invasive ductal carcinoma. Tissues expressing miR-149 or GIT1 at levels lower than median  $-1$  s.d. levels were assigned to the low (miR-149,  $n=61$ ; GIT1,  $n=64$ ) and those above the median  $+1$  s.d. level were assigned to the high (miR-149,  $n=65$ ; GIT1,  $n=64$ ) expression group. On the basis of the clinical staging, we found that the late stages had lower miR-149 ( $P=0.03$ ) and higher GIT1 ( $P=0.03$ ) expression in comparison with the early-stage breast cancer (Tables 1 and 2). However, there

were no significant differences in miR-149 and GIT1 expression between tumors and adjacent normal tissues (Supplementary Figure 17).

We next assessed the expression of miR-149 and GIT1 using 26 pairs of primary breast tumors and lymph node metastases from the same patients. The result of qRT-PCR showed that miR-149 was significantly downregulated in most lymph node metastases (16/26, 61%) compared with their paired primary tumors ( $P=0.03$ ; Figure 8a). Conversely, GIT1 was upregulated in most lymph node metastases (18/26, 69%) compared with the paired primary tumors ( $P=0.003$ ; Figure 8b). Moreover, we found that miR-149 expression was negatively correlated with GIT1 expression in those specimens ( $P < 0.01$ ; Figure 8c).

To confirm the above finding using a different cohort, we performed fluorescent *in situ* hybridization (FISH) and immunohistochemistry (IHC) on commercial tissue array containing nine pairs of matched primary tumors and lymph node metastases. FISH data showed that seven out of nine (77%) lymph node metastases expressed lower level of miR-149 compared with the matched primary tumors (Figures 8d and e). IHC data revealed that six out of nine (66%) lymph node metastases expressed higher level of GIT1 in comparison with the matched primary tumors (Figures 8d and f). The result showed that six out of nine pairs (66%) followed the expected miR-149-GIT1 regulation pattern (as indicated by the red dots below the histogram) where metastatic tumors showed lower level of miR-149 and higher level of GIT1 when compared with the matched primary tumors (Figures 8d and e).

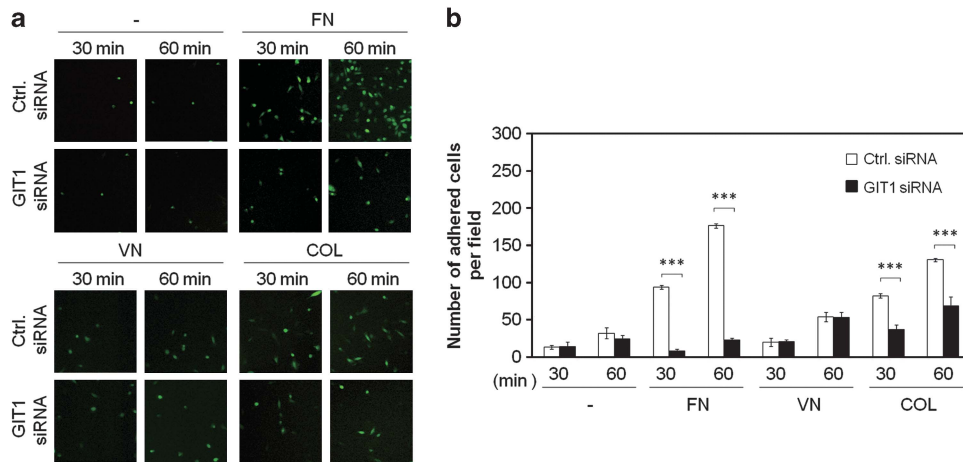


**Figure 7.** GIT1 depletion greatly reduces  $\alpha 5\beta 1$ -integrin-mediated cell adhesion to fibronectin in metastatic IV2 cells. **(a)** Representative photographs of the adhered GFP-tagged IV2-1 cells from different time points under different coating conditions. **(b)** Quantitative data are shown by histograms. The GFP-tagged IV2-1 cells were transfected with GIT1 siRNA and the control (Ctrl) siRNA. The transfected cells were then seeded on fibronectin (FN)-, vitronectin (VN)- and type IV collagen (COL)-coated 3.5-cm dishes, and the unadhered cells were washed out with after 30 and 60 min. The photo was taken under  $\times 100$  microscope. All experiments were performed in triplicates in each experiment and repeated three times. \*\*\* $P < 0.001$  compared withCtrls.

**Table 1.** The level of miR-149 expression is correlated with clinical stage of breast cancer patients

miR-149	Stage		Fisher's exact test $P = 0.03$
	I and II (n = 70)	III and IV (n = 56)	
High expression <sup>a</sup> (n = 65)	41	24	
Low expression <sup>b</sup> (n = 61)	29	32	

Abbreviation: miR, microRNA. <sup>a</sup>miR-149 level was higher than median+1 s.d. (1.8+0.25). <sup>b</sup>miR-149 level was lower than median - 1 s.d. (1.8 - 0.25).

**Table 2.** The GIT1 expression is correlated with clinical stage of breast cancer patients

GIT1	Stage		Fisher's exact test $P = 0.03$
	I and II (n = 67)	III and IV (n = 61)	
High expression <sup>a</sup> (n = 64)	28	36	
Low expression <sup>b</sup> (n = 64)	39	25	

Abbreviation: GIT1, G-protein-coupled receptor kinase-interacting protein 1. <sup>a</sup>GIT1 level was higher than median+1 s.d. (0.095+0.012). <sup>b</sup>GIT1 level was lower than median - 1 s.d. (0.095-0.012).

Taken together, analysis of clinical samples indicated that miR-149-GIT1 regulation axis is involved specifically in breast cancer progression and lymph node metastasis.

## DISCUSSION

In the present study, we have identified miR-149 as a negative regulator of breast cancer cell migration, invasion and metastasis by targeting GIT1 expression (see Figure 9). Our study is the first to explore the role of miR-149 in breast cancer metastasis. We have demonstrated the relevance of miR-149 in clinical malignancies in that low expression of miR-149 and high expression of GIT1 is significantly associated with advanced stages and lymph node metastasis in breast cancer patients. We demonstrated that miR-149 mediates inhibition of metastasis via modulating pathways directly affecting cell migration and invasion. We also showed that miR-149 has a crucial role in intervening lung targeting ability of metastatic breast cancer cells. As such, miR-149 could be classified in the category of metastasis suppressor gene.

Recently, other groups have reported the differential expression of miR-149 in other types of cancers.<sup>19-21</sup> The miR-149 was reported to be downregulated in astrocytomas<sup>20</sup> and upregulated in nasopharyngeal carcinoma<sup>19</sup> by microarray screening. In gastric cancer, miR-149 was reported to function as a tumor suppressor

that inhibits cell cycle progression of cancer cells by targeting *ZBTB2*.<sup>21</sup> Our data show that miR-149 is downregulated in advanced and metastatic breast cancers by targeting migration and invasion-related genes (Figure 8). Taken together with previous studies, it suggests that miR-149 can be multitasking by regulating different downstream effectors in different cancer contexts and it functions mainly as a metastasis suppressor in breast cancer.

Our functional study shows that GIT1 is a downstream target and effector of miR-149. Knockdown of GIT1 expression reduced *in vitro* cell migration and invasion of IV2 and Hs578T cells (Figures 4a and b and Supplementary Figure 14). However, in our cell-based and mouse model studies, re-expression of GIT1 could significantly but not completely reverse the miR-149-imposed inhibition on invasion/metastasis (Figures 4c-f), suggesting that other potential targets of miR-149 may exist. Our data provide the first and direct evidence that GIT1 has an important role in breast cancer metastasis. Interestingly, in a separate study, we found that GIT1 also played an important role in lymph node metastasis of oral squamous cell carcinoma (WC Huang *et al.*, unpublished).

Our investigation of the downstream effector(s) of miR-149-GIT1 signaling axis showed that downregulation of GIT1 could impair the activation of FAK (autophosphorylation at Y397) upon fibronectin-integrin engagement and subsequent FAK-Src



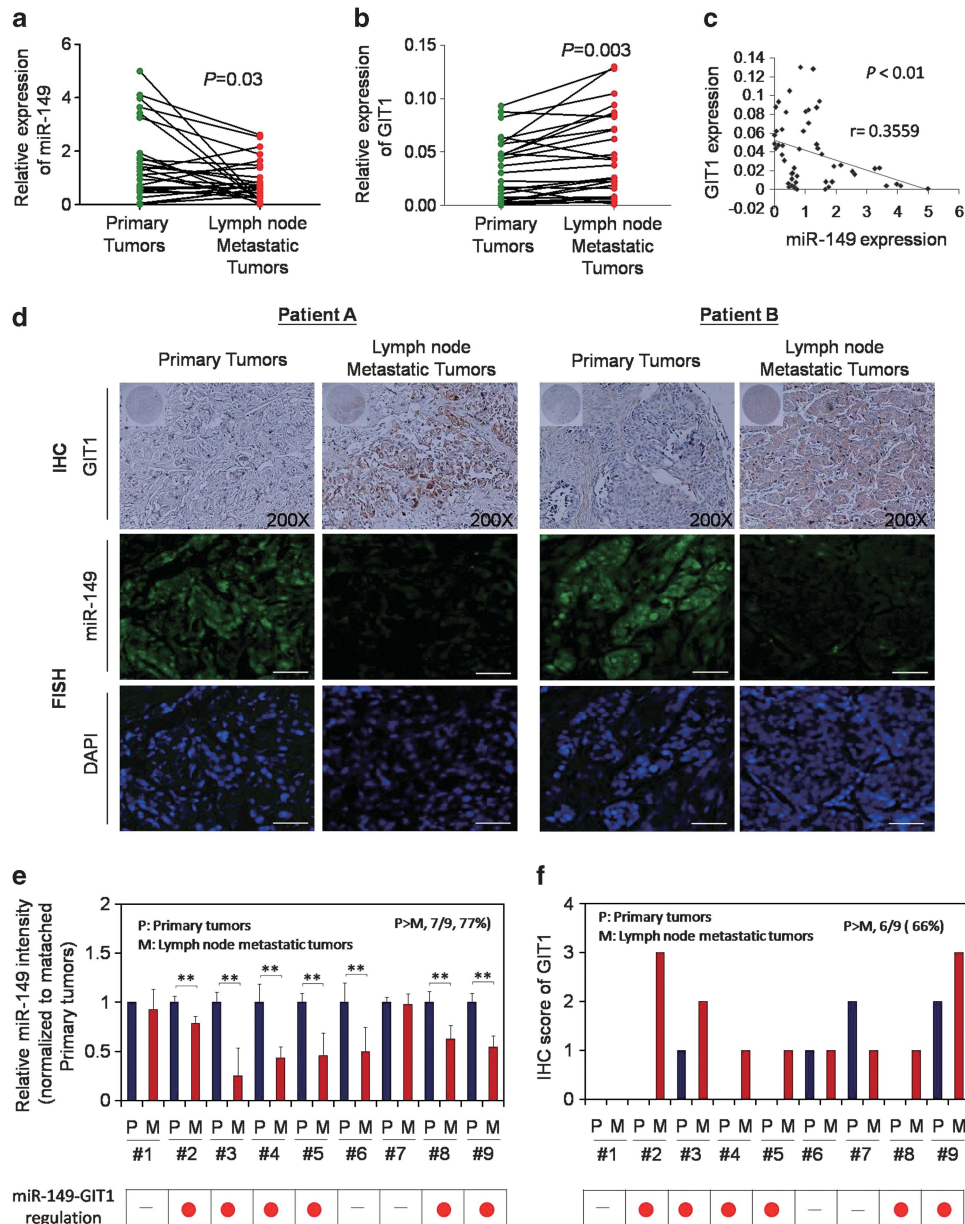


**Figure 8.** Low level of miR-149 and high level of GIT1 correlate with lymph node metastasis. **(a and b)** qPCR analysis of miR-149 and GIT1 levels in paired primary tumors and lymph node metastases from 26 patients. **(c)** Correlation analysis of miR-149 and GIT1. **(d)** Analysis of miR-149 and GIT1 protein expression in paired primary tumors and lymph node metastases from commercial tissue array using FISH and IHC, respectively. **(e)** Semiquantification of fluorescence intensity of miR-149 from each specimen is shown by histograms. **(f)** IHC score of GIT1 from each specimen is shown by histograms. The expected miR-149-GIT1 regulation pattern was indicated by the red dots below the histogram. Scale bar: 50  $\mu\text{m}$ .  $**P < 0.01$  compared with primary tumors.

signaling, including FAK phosphorylation at Y861 and paxillin phosphorylation at Y118 (Figure 5), both are well-known substrates for Src kinase.<sup>22,23</sup> Furthermore, our study reveals that loss of GIT1 causes protein instability of  $\alpha 5\beta 1$  integrin complexes through lysosomal degradation (Figure 6). As integrin-mediated formation of focal adhesion is the major upstream activator of FAK, downregulation of the  $\alpha 5\beta 1$  integrin provides an explanation of how FAK-Src signaling could be impaired in the absence of GIT1. In addition, we observed that the reduction of paxillin phosphorylation at Y118 in the absence of GIT1 was not only because of impaired FAK-Src signaling but also in part because of increased proteasomal degradation of paxillin, leading to its instability (Figure 6). Given that GIT1 can interact, through its paxillin-binding domain, with paxillin to sequester its location at

focal adhesion points, we reason that losing contact with GIT1, resulting in increased protein instability of paxillin, could be another explanation for the disruption of focal adhesions. Our study unravels a novel function of GIT1 in stabilizing  $\alpha 5\beta 1$  integrin and adaptor molecule, paxillin, of focal adhesion complexes, perhaps by localized sequestration, and thus, preventing them from protein degradation (see Figure 9). We also found that GIT1 is important for  $\alpha 5\beta 1$ -integrin-mediated cell adhesion to fibronectin and collagen.

The clinical relevance of GIT1 in human malignancies has not been reported before. Our clinical data reveal the first indication that that high level of GIT1 is correlated with advanced stages and lymph node metastasis of breast cancer (Tables 1 and 2 and Figure 8). Our overall data show that the miR-149-GIT1 signaling

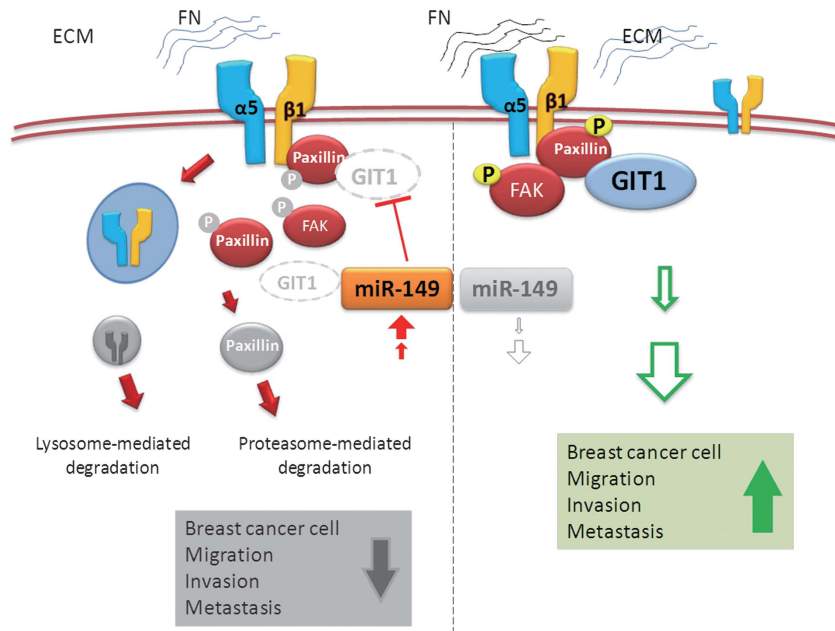


**Figure 9.** Model of miR-149-GIT1 regulation pathways in regulating breast cancer metastasis. (Left) Under conditions of high miR-149, as in non-invasive breast cancer cells, GIT1 protein levels are reduced, leading to changes in focal adhesion protein (cell surface  $\alpha 5$  and  $\beta 1$  integrin and intracellular paxillin) stability and function that favors low migratory and metastatic potential. (Right) Under conditions of low miR-149, GIT1 levels rise, stabilizing integrin and paxillin proteins and promoting high adhesion, migration and metastasis. ECM, extracellular matrix; FN, fibronectin.

axis is important for regulating metastasis during breast cancer progression.

In addition, GIT1 has also been shown to form a multisubunit complex with paxillin, PIX and PAK to promote cell migration and lamellipodia formation, which is known to be regulated by the small GTPase such as Rac1/Cdc42.<sup>24</sup> Therefore, the level of PIX and PAK and the activity of Rac1/cdc42 in GIT1-depleted metastatic IV2 cells will be examined in the future study.

Our present study has identified a novel metastasis suppressor miRNA, miR-149, in breast cancer that can negatively regulate GIT1 *in vitro* and *in vivo*. Taken together with clinical observations, our finding suggests that miR-149 and GIT1 are significant biomarkers for metastasis and could be targets for the development of antimetastasis strategy in the treatment of breast cancer.

## MATERIALS AND METHODS

### Cell culture

MCF-7, T-47D, SK-BR-3, BT-549, Hs578T, MDA-MB-231 and MDA-MB-453 were obtained from ATCC (Manassas, VA, USA) and were cultured in Dulbecco's modified Eagle's medium supplemented with 10% fetal bovine serum (Invitrogen, Carlsbad, CA, USA).

### *In vivo* selection of highly metastatic breast cancer cells

Detailed procedure was described in Supplementary Figure 1.

### RNA extraction and qRT-PCR

Detailed procedures of RNA extraction and qRT-PCR were described elsewhere.<sup>25</sup> Specific primers used in this experiment are described in Supplementary Table 3.

### miRNA array analysis

The miRNA expression pattern between the MDA-MB-231 parental cells and three *in vivo*-selected lung metastatic IV2 sublines were analyzed using Affymetrix miRNA 2.0 array (Affymetrix, Santa Clara, CA, USA). The miRNA array experiment was carried out at Microarray Core Laboratory in National Health Research Institute (Miaoli, Taiwan).

### Patients and tissue samples

Two hundred and nine cancer samples and 50 adjacent normal tissues were collected according to National Taiwan University Hospital, Chi Mei Medical Center and Chiayi Christian Hospital Institutional Review Board-approved guidelines. Commercial breast carcinoma tissue array slides were purchased from US Biomax Inc. (Rockville, MD, USA).

### Antibodies and reagents

Detailed information of antibodies and reagents used in this study is provided in Supplementary Table 4.

### Focal adhesion assay and immunofluorescent staining

A total of  $5 \times 10^4$  IV2 cells were seeded on 10  $\mu\text{g}/\text{ml}$  FN-coated coverslips for 90 min in complete medium, and then fixed, permeabilized, blocked and stained with anti-vinculin (Sigma-Aldrich Inc., St Louis, MO, USA) antibody as described previously.<sup>26</sup> Samples were observed and photographed using the Leica SP5 II scanning confocal microscope (Leica, Bannockburn, IL, USA). Focal adhesion areas were determined by measuring pixel areas above an empirically determined background threshold of fluorescence intensity using the ImageJ software (NIH, Bethesda, MD, USA).

### Western blotting

Detailed procedure was described elsewhere.<sup>25</sup>

### Migration and invasion assay

Migration and invasion assays were carried out using 8.0  $\mu\text{m}$  Falcon Cell Culture with or without the Matrigel (BD Biosciences, San Jose, CA, USA) as described previously.<sup>25</sup>

### Cell adhesion assays

A total of  $5 \times 10^5$  cells were seeded on fibronectin-, vitronectin- and type IV collagen-coated 3.5-cm dishes. Detailed procedure was described elsewhere.<sup>27</sup>

### In vivo metastasis assay

A total of  $1 \times 10^6$  IV2 cells with indicated treatments were suspended in 100  $\mu$ l phosphate-buffered saline and injected individually into the tail veins of C.B-17 severe-combined immunodeficient mice. After 45 days, mice were killed, lung tissues were dissected and subjected to histological examination (see below). The C.B-17 severe-combined immunodeficient mice were provided by the National Laboratory Animal Center (Taipei, Taiwan). All animal studies were approved by Institutional Animal Care and Use Committee (IACUC) of National Health Research Institute.

### Histological analysis

For examination of lung metastasis in mice, lungs were fixed in 4% formaldehyde overnight and were embedded in paraffin. Six-micrometer-thick sections were prepared and stained with H&E.

### 3'-UTR luciferase reporter assay

Cells were harvested at 48 h after transfection. Luciferase activity was measured according to the manufacturer's instruction (Promega, Madison, WI, USA). The luciferase activity was normalized to  $\beta$ -galactosidase activity.

### Establishment of stable cell lines and plasmid construction

Green fluorescent protein (GFP)-tagged IV2-1 cells were generated by transfection with pcDNA6.2-GW-EmGFP plasmid, and subsequently by blasticidin selection. miR-con-s and miR-149-s stable lines were generated by transfection of pcDNA-GW control vector or pcDNA-GW-miR-149 plasmid into IV2-1 cells, respectively. The human GIT1 cDNA (770-amino-acid form) was amplified with gene-specific primers from IV2 cell-derived RNAs by PCR and cloned into pCMV-HA (Clontech, Mountain View, CA, USA). The R39K GIT1 mutant was generated by site-directed mutagenesis. The wild-type GIT1 3'-UTR was cloned by PCR into pGL3-SV40 (Promega) using specific primers. The mutant GIT1 3'-UTR was generated by site-directed mutagenesis. The miR-149 expression construct pcDNA6.2-GW-miR-149 was purchased from Invitrogen. The miR-149 sponge plasmid was designed according to a previous study.<sup>28</sup> Briefly, oligonucleotides containing seven miR-149 binding sites with 4-nucleotide spacer were annealed and cloned into pEGFP-C1 (Clontech). The sequences of primers and sponge oligonucleotides described above are listed in Supplementary Table 3.

### Plasmid and oligonucleotide transfection

Cells were transfected with appropriate plasmids using Lipofectamine 2000 (Invitrogen). For siRNA and miRNA transfection, Lipofectamine RNAiMAX (Invitrogen) was used. The pre-miR-149 was purchased from Applied Biosystems (Beverly, MA, USA). The anti-miR-149 was purchased from GeneDireX Inc. (Las Vegas City, NV, USA). GIT1 siRNA was purchased from MDBio Inc. (Taipei, Taiwan).

### Protein degradation assay

Cells were treated with 10  $\mu$ g/ml cycloheximide for the indicated times and then harvested in RIPA buffer containing protease inhibitors (Roche, Madison, WI, USA) for western blotting analysis.

### IHC and FISH

Immunohistochemical staining was carried out as the published procedure using anti-GIT1 antibody (Bethyl Labs, Montgomery, TX, USA).<sup>29</sup> FISH of miRNA was performed according to a previous study.<sup>30</sup> The biotin-labeled miR-149 probe was purchased from GeneDireX Inc. The result of IHC and FISH was independently scored by two investigators in a double blind manner. The histological score of GIT1 for each specimen was graded as follows: 0, negative; 1, weak; 2, moderate; 3, strong. The fluorescence intensity of miR-149 of each specimen was semiquantitatively determined using the ImageJ software.

### Statistical analysis

Data are presented as mean  $\pm$  s.e.m. Student's *t*-test was used for comparison. The differences in the expression level of miR-149 and GIT1 in breast carcinoma tissues of different stages were calculated using the Fisher's exact probability test. The differences in the expression level of miR-149 and GIT1 between primary breast carcinoma and lymph node

metastases were calculated using paired *t*-test. Differences were considered significant at  $P < 0.05$  (\* $P < 0.05$ , \*\* $P < 0.01$  and \*\*\* $P < 0.001$ ). NS represents no significance.

### CONFLICT OF INTEREST

The authors declare no conflict of interest.

### ACKNOWLEDGEMENTS

We thank the Pathology Core Laboratory and Microarray Core Laboratory of the National Health Research Institutes for H&E and immunohistochemical staining and miRNA array analysis, respectively. This work was supported by grants from National Science Council, Taiwan (01D2-MMNSC16) and the Department of Health, Taiwan (DOH100-TD-111-004).

### REFERENCES

- Gupta GP, Massague J. Cancer metastasis: building a framework. *Cell* 2006; **127**: 679–695.
- Steege PS. Tumor metastasis: mechanistic insights and clinical challenges. *Nat Med* 2006; **12**: 895–904.
- Schuldt A. Micromanaging metastasis. *Nat Cell Biol* 2007; **9**: 1121.
- Zhang J, Ma L. MicroRNA control of epithelial–mesenchymal transition and metastasis. *Cancer Metastasis Rev* 2012; **31**: 653–662.
- Sreekumar R, Sayan BS, Mirnezami AH, Sayan AE. MicroRNA control of invasion and metastasis pathways. *Front Genet* 2011; **2**: 58–62.
- Negrini M, Calin GA. Breast cancer metastasis: a microRNA story. *Breast Cancer Res* 2008; **10**: 203–206.
- Guo W, Giancotti FG. Integrin signalling during tumour progression. *Nat Rev Mol Cell Biol* 2004; **5**: 816–826.
- White DE, Muller WJ. Multifaceted roles of integrins in breast cancer metastasis. *J Mamm Gland Biol Neo* 2007; **12**: 135–142.
- Desgrosellier JS, Cheresh DA. Integrins in cancer: biological implications and therapeutic opportunities. *Nat Rev Cancer* 2010; **10**: 9–22.
- Ramsay AG, Marshall JF, Hart IR. Integrin trafficking and its role in cancer metastasis. *Cancer Metast Rev* 2007; **26**: 567–578.
- Hood JD, Cheresh DA. Role of integrins in cell invasion and migration. *Nat Rev Cancer* 2002; **2**: 91–100.
- Schlenker O, Rittinger K. Structures of dimeric GIT1 and trimeric beta-PIX and implications for GIT–PIX complex assembly. *J Mol Biol* 2009; **386**: 280–289.
- Manabe R, Kovalenko M, Webb DJ, Horwitz AR. GIT1 functions in a motile, multi-molecular signaling complex that regulates protrusive activity and cell migration. *J Cell Sci* 2002; **115**: 1497–1510.
- Schmalzigaug R, Garron ML, Roseman JT, Xing Y, Davidson CE, Arold ST et al. GIT1 utilizes a focal adhesion targeting-homology domain to bind paxillin. *Cell Signal* 2007; **19**: 1733–1744.
- Yin G, Zheng Q, Yan C, Berk BC. GIT1 is a scaffold for ERK1/2 activation in focal adhesions. *J Biol Chem* 2005; **280**: 27705–27712.
- Luo M, Guan JL. Focal adhesion kinase: a prominent determinant in breast cancer initiation, progression and metastasis. *Cancer Lett* 2010; **289**: 127–139.
- Liu S, Calderwood DA, Ginsberg MH. Integrin cytoplasmic domain-binding proteins. *J Cell Sci* 2000; **113**: 3563–3571.
- Hunziker W, Geuze HJ. Intracellular trafficking of lysosomal membrane proteins. *BioEssays* 1996; **18**: 379–389.
- Luo Z, Zhang L, Li Z, Li X, Li G, Yu H et al. An *in silico* analysis of dynamic changes in microRNA expression profiles in stepwise development of nasopharyngeal carcinoma. *BMC Med Genom* 2012; **5**: 3.
- Li D, Chen P, Li XY, Zhang LY, Xiong W, Zhou M et al. Grade-specific expression profiles of miRNAs/mRNAs and docking study in human grade I–III astrocytomas. *OMICS* 2011; **15**: 673–682.
- Wang Y, Zheng X, Zhang Z, Zhou J, Zhao G, Yang J et al. MicroRNA-149 inhibits proliferation and cell cycle progression through the targeting of ZBTB2 in human gastric cancer. *PLoS One* 2012; **7**: e41693.
- Calalb MB, Zhang X, Polte TR, Hanks SK. Focal adhesion kinase tyrosine-861 is a major site of phosphorylation by Src. *Biochem Biophys Res Commun* 1996; **228**: 662–668.
- Parsons JT, Horwitz AR, Schwartz MA. Cell adhesion: integrating cytoskeletal dynamics and cellular tension. *Nat Rev Mol Cell Biol* 2010; **11**: 633–643.
- Ridley AJ, Schwartz MA, Burridge K, Firtel RA, Ginsberg MH, Borisy G et al. Cell migration: integrating signals from front to back. *Science* 2003; **302**: 1704–1709.
- Lin KT, Gong J, Li CF, Jang TH, Chen WL, Chen HJ et al. Vav3-rac1 signaling regulates prostate cancer metastasis with elevated Vav3 expression correlating

- with prostate cancer progression and posttreatment recurrence. *Cancer Res* 2012; **72**: 3000–3009.
- 26 Thievensen I, Thompson PM, Berlemont S, Plevock KM, Plotnikov SV, Zemljic-Harpf A *et al*. Vinculin–actin interaction couples actin retrograde flow to focal adhesions, but is dispensable for focal adhesion growth. *J Cell Biol* 2013; **202**: 163–177.
- 27 Narla RK, Chen CL, Dong Y, Uckun FM. *In vivo* antitumor activity of bis(4,7-dimethyl-1,10-phenanthroline) sulfatoxovanadium(IV) (METVAN [VO(SO<sub>4</sub>)(Me<sub>2</sub>-Phen)<sub>2</sub>]). *Clin Cancer Res* 2001; **7**: 2124–2133.
- 28 Ebert MS, Neilson JR, Sharp PA. MicroRNA sponges: competitive inhibitors of small RNAs in mammalian cells. *Nat Methods* 2007; **4**: 721–726.
- 29 Packeisen J, Buerger H, Krech R, Boecker W. Tissue microarrays: a new approach for quality control in immunohistochemistry. *J Clin Pathol* 2002; **55**: 613–615.
- 30 Silaharoglu AN, Nolting D, Dyrskjot L, Berezikov E, Moller M, Tommerup N *et al*. Detection of microRNAs in frozen tissue sections by fluorescence *in situ* hybridization using locked nucleic acid probes and tyramide signal amplification. *Nat Protoc* 2007; **2**: 2520–2528.



This work is licensed under a Creative Commons Attribution-NonCommercial-ShareAlike 3.0 Unported License. To view a copy of this license, visit <http://creativecommons.org/licenses/by-nc-sa/3.0/>

Supplementary Information accompanies this paper on the Oncogene website (<http://www.nature.com/onc>)